THE JOURNAL OF BIOLOGICAL CHEMISTRY
Vol. 277, No. 34, Issue of August 23, pp. 30606–30613, 2002
Printed in U.S.A.

Specific Cleavage of Hepatitis C Virus RNA Genome by Human RNase P*

Received for publication, April 15, 2002, and in revised form, June 6, 2002
Published, JBC Papers in Press, June 11, 2002, DOI 10.1074/jbc.M203595200

Anna Nadal‡, María Martell‡, J. Robin Lytle§, Alita J. Lyons§, Hugh D. Robertson§, Beatriz Cabot‡, Juan I. Esteban‡, Rafael Esteban‡, Jaime Guardia‡, and Jordi Gómez‡¶

From the ‡Servicio de Medicina Interna-Hepatología, Area de Investigación Básica, Hospital Valle de Hebrón, Barcelona 08035, Spain and the §Department of Biochemistry, Weill Medical College of Cornell University, New York, New York 10021

We have found that RNase P from HeLa cells specifically and efficiently cleaves hepatitis C virus (HCV) transcripts *in vitro*. The evidence includes identification of the 5′-phosphate polarity of the newly generated termini at position A^{2860} as well as immunological and biochemical assays. Active cleavage has been shown in five dominant sequences of HCV "quasispecies" differing at or near the position of cleavage, demonstrating that this is a general property of HCV RNA. During the analysis, a second cleavage event was found in the 3′ domain of the internal ribosome entry site. We have found that HCV RNA competitively inhibits pre-tRNA cleavage by RNase P, suggesting that HCV RNA has structural similarities to tRNA. This finding sets HCV apart from other pathogens causing serious human diseases and represents the first description of human RNase P-viral RNA cleavage. Here we discuss the possible meaning of these RNase P-accessible structures built into the viral genome and their possible role *in vivo*. Moreover, such structures within the viral genome might be vulnerable to attack by therapeutic strategies.

Hepatitis C virus (HCV)[1] is a human pathogen causing chronic liver disease in 170 million people worldwide. The virus is classified within the family *Flaviviridae* (1). The RNA genome is single-stranded and functions as the sole mRNA species for translation (1) (Fig. 1*A*). It comprises a 5′-untranslated region, which functions as an internal ribosome entry site (IRES) (2), and a long open reading frame, which encodes a polyprotein precursor of about 3010 amino acids, that is cleaved into structural (core, envelope 1, envelope 2, and p7) and nonstructural (NS-2, NS-3, NS-4, and NS-5) proteins (3), followed by a 3′-noncoding region (4).

Analyzing significant numbers of cDNA clones of hepatitis C virus from single isolates provides unquestionable proof that the viral genome cannot be defined by a single sequence but rather by a population of variant sequences closely related to one another (5–7). In the infected patient, a master (the most frequently represented sequence) and a spectrum of mutant sequences (diverging by up to 5%) may be isolated at any given time during chronic infection (7). This manner of organizing genetic information, which characterizes most RNA viruses, is referred to as "quasispecies" (8). It has been proven that the use of this strategy provides RNA viruses with a rapid increase of fitness while growing in cell culture conditions (9).

Many studies on genetic variability in recent years have focused on the analysis of HCV quasispecies. Clinically relevant features, such as the ability to produce chronic infections and severity of disease (including the frequency of hepatocellular carcinoma), have been related to the interplay between host influences and the array of viral variants in each infected individual (10). HCV resistance to interferon treatment (either alone or in combination with ribavirin) is one of the most important clinical implications predicted by the quasispecies model (11–14), suggesting the necessity to seek new therapies. HCV therapeutic strategies based on ribozyme cleavage are leading candidates. It may be argued that a sequence-dependent ribozyme designed to cleave viral RNA by interaction with a motif in the viral RNA may, in fact, select for (mismatching) variants resistant to the ribozyme. However, strategies could be designed to take advantage of ribozyme capabilities to minimize the effect of virus variability. Combination therapy with multiple ribozymes directed against independent viral loci has been demonstrated to be efficient in inhibiting influenza virus replication in cell culture (15). Making conserved motifs within the viral genome accessible to therapy, as in the case of the HCV IRES, could be another promising strategy.

The ribozyme activity of RNase P is among proposed antiviral agents (16). RNase P is a ubiquitous cellular endonuclease and one of the most abundant and efficient enzymes in the cell. This enzyme is a ribonucleoprotein complex that catalyzes a hydrolysis reaction to remove the leader sequence of precursor tRNA (pre-tRNA) to generate the mature tRNA (17). RNase P from *Escherichia coli* contains a catalytic RNA subunit termed M1 RNA and a single polypeptide known as C5 protein (18). In the presence of a high concentration of Mg^{2+}, M1 RNA itself can hydrolyze tRNA precursors *in vitro* (19). Human RNase P also contains an RNA subunit, H1 RNA, but in the absence of protein factors, H1 RNA does not exhibit enzymatic activity by itself *in vitro* (20, 21). Substrate recognition by the RNase P ribozyme does not rely on sequence requirements but on structural features of the RNA substrate. Custom-designed ribo-oligonucleotides, which hybridize with the target, called external guide sequences, may

* Work in New York was supported by National Institutes of Health Grant DK-56424. Work in Barcelona was funded by Ministerio de Ciencia y Tecnología Grants SAF1999-0108 and BIO00-0347, Ministerio de Sanidad y Consumo Grant FISS-01/1351, and the Hospital Vall d'Hebron. The costs of publication of this article were defrayed in part by the payment of page charges. This article must therefore be hereby marked "*advertisement*" in accordance with 18 U.S.C. Section 1734 solely to indicate this fact.

¶ To whom correspondence and requests for materials should be addressed: Laboratorio de Medicina Interna-Hepatología, Area de Investigación Básica (B), Hospital Vall d′Hebron, Paseo Vall d′Hebrón 119-129, Barcelona 08035, Spain. Tel.: 34-93-4894034; Fax: 34-93-4894032; E-mail: jgomez@hg.vhebron.es.

[1] The abbreviations used are: HCV, hepatitis C virus; nt, nucleotide(s); IRES, internal ribosome entry site; pre-tRNA, precursor tRNA; HBV, hepatitis B virus.

provide the RNA structure that RNase P recognizes and cleaves in the hybridized complex (16).

Recognition of structures instead of sequences may represent a great advantage in the fight against variable viruses, because single or even double mutations in the target may be tolerated for RNase P recognition (15). Also, it has already been shown that some forms of the catalytic RNA moiety from *E. coli* RNase P, M1 RNA (either specifically modified or *in vitro* selected), can be introduced into the cytoplasm of mammalian cells for the purpose of carrying out targeted cleavage of mRNA molecules (22, 23).

While performing targeting experiments on HCV RNA transcripts with RNase P, we have found that, surprisingly, purified RNase P (peak activity) from HeLa cells cleaved HCV genomic RNA efficiently at two sites in the absence of external guide sequences. We report here the techniques used to prove that the cleavage is specific to human RNase P and to show where cleavage occurs. We further report that cleavage is maintained in several variant sequences, which makes RNase P cleavage an inherent property of HCV RNA. Since RNase P recognizes and cleaves tRNA-like structures, these results suggest the presence of tRNA-like structures within the viral genome.

EXPERIMENTAL PROCEDURES

Preparation of RNA Transcripts—RNA transcripts used as substrates in the human RNase P assays were derived from plasmids pN(1–4728) Bluescript, which contains nt 1–4728 of hepatitis C virus under the T7 promoter, and pUC19 TyrT, which contains the sequence of the naturally occurring precursor to $tRNA^{Tyr}$. To obtain the radioactive substrates for peak RNase P activity from HeLa cells, 1–2-μg DNA templates were transcribed *in vitro* (1 h at 37 °C) with [α-^{32}P]GTP or [α-^{32}P]NTPs followed by a 5-min treatment with RNase-free DNase I at 37 °C. We used cellulose CF11 chromatography to eliminate DNA fragments and nonincorporated nucleotides. Transcripts were then purified by gel electrophoresis under denaturing conditions on 4% polyacrylamide gels containing 7 M urea. Bands were visualized by autoradiography, excised from the gel, and eluted in buffer (100 mM Tris-HCl, pH 7.5, and 10 mM EDTA, pH 7.5). The concentration of radioactive transcripts was determined by calculating the amount of incorporated [α-^{32}P]GTP based on scintillation counting.

Partial Purification of Human RNase P—RNase P was purified from 30 g of HeLa cells according to the method of Bartkiewicz *et al.* (20) with some modifications. Fractions eluted with a linear gradient of 100–350 mM from a column of DEAE-Sepharose CL-6B (bed volume, 150 ml) were tested to determine (i) enzymatic activity using pre-$tRNA^{Tyr}$ as substrate and (ii) the presence of the H1 RNA moiety from RNase P but also the presence of RNA from MRP RNase, which could co-extract with RNase P during the purification protocol. H1 RNA and MRP RNA were quantified by using Taqman technology (Roche Molecular Biochemicals) and real time reverse transcriptase-PCR (Abi Prism 7700, PE Biosystems) following the protocol used for the quantification of HCV RNA from human serum or liver samples (24) (data not shown). We have used one set of specific human RNase P primers (PH1–213, 5′-CCCGGCGGATGCCT-3′; PH1–274, 5′-TTGAACTCACTTCGCTGGCC-3′) and a fluorogenic probe (PH1–228, 5′-(VIC; Applied Biosystems) CTTTGCCGGAGCTTGGAACAGACTCA(6-carboxy-tetramethylrhodamine)-3′) and a second set of specific human MRP primers (MRP-90, 5′-AGAGAGTGCCACGTGCATACG-3′; MRP-210, 5′-TAACTAGAGGGAGCTGACGGATG-3′) and a fluorogenic probe labeled with a different reporter (MRP-145, 5′-(6-carboxy fluorescein)CGCCAAGAAGCGTATCCCGCTGA(6-carboxy-tetramethylrhodamine)-3′). Relative quantitation of both RNase P RNA and MRP RNA was performed by comparing the amplification results for the different fractions with those on standard curves generated from serial dilutions of total RNA extracted from HeLa cells. Using the purification protocol described above, RNase P and MRP co-extracted together but with an enrichment of RNase P *versus* MRP of several orders of magnitude, in all of the tested fractions (3.3×10^{11} molecules of RNase P RNA *versus* 8.2×10^{7} molecules of MRP RNA, on average, in the fractions from the ammonium chloride gradient).

Fractions with coincident peaks of enzymatic activity and H1 RNA amplification were pooled and concentrated, using the Millipore Ultrafree-15 centrifugal filter device, to a final volume of ~6 ml. The concentrated fractions were subjected to linear glycerol gradient centrifugation, as described (20). Relative quantitation of RNase P and MRP RNA molecules at this point confirmed previous results (*i.e.* enrichment of RNase P *versus* MRP during the purification process (6.7×10^{10} molecules of RNase P RNA *versus* 6.7×10^{7} molecules of MRP RNA, on average, in the fractions from the glycerol gradient)). Again, fractions containing the peak of enzymatic activity were concentrated to a final volume of 0.1 ml and stored at −70 °C.

RNase P Cleavage Assay—Substrates for RNase P assays, S_I, S_{II}, S_{III}, and S_{IV} transcripts (1.8 nM final concentration) were preheated at 90 °C for 1 min before the addition of reaction buffer (10 mM HEPES-KOH, pH 7.5, 10 mM MgOAc, 100 mM NH_4OAc) and left to cool to room temperature. Cleavage reactions were performed with 4% polyethylene glycol, 20 units of RNasin, and 2 μl of the RNase P peak activity and carried out at 30 °C in a volume of 10 μl for 30 min. Samples were subjected to 2% SDS and 5 min at 60 °C to disrupt aggregates before loading. Cleavage products were separated on 4% denaturing polyacrylamide gels and visualized by autoradiography.

Determination of Cleavage Site and Phosphate Polarity—Oligonucleotides released from RNase T1 digestions of all four single or mixed labeled S_I, 5′ P_I, and 3′ P_I RNAs were fractionated to yield two-dimensional fingerprints (first separation by gel electrophoresis and second by homochromatography) exactly as described (25). Standard conditions for secondary analysis (with pancreatic RNase A, RNase U2, RNase T2, or 0.4 M NaOH) (26) were followed permitting the oligonucleotides to be identified. One-dimensional electrophoresis on DEAE or 3MM paper was done following Barrells' protocol (26).

Immunoprecipitation of RNase P Activity—Serum containing anti-Th antibodies from a patient with an autoimmune disease was used to immunodeplete RNase P activity (27). Protein A-Sepharose beads (125 μg, dry weight; Amersham Biosciences) were washed with TMKT buffer (10 mM Tris-HCl, pH 7.5, 10 mM $MgCl_2$, 100 mM KCl, 0.02% Tween 20) before incubation for 1 h at room temperature at different concentrations of either normal serum or anti-Th serum (0.25, 0.5, or 1 μl) and in 30 μl of TMKT buffer. After washing four times in TMKT, followed by three washes in RNase P buffer (10 mM HEPES-KOH, pH 7.5, 10 mM MgOAc, 100 mM NH_4OAc), the beads were incubated for 2 h at 4 °C in 2.5 μl of RNase P extract. The suspension was centrifuged, and both the supernatant and the immunoprecipitate were assayed for enzyme activity. To facilitate migration of products on the acrylamide gel, an additional step of proteinase K treatment was carried out after phenol/SDS treatment on each reaction tube.

Construction of Plasmids Containing HCV Variants—HCV variants were obtained from our library of cloned fragments encompassing HCV nucleotides 2641–2872 from infected patients. Subsequently the fragments were extended by PCR at their 3′-ends using primers HCV-2639 (5′-ACAGGATCCAGTCCTTCCTTGTGTTCTTCT-3′) and HCV-2871 (5′-AACGAATTCCCACACATGCAAGTGCGCCTCAGCTCTGGTGATAAGATATTGTAACCACCA-3′), corresponding to the "wild type" clone (this length of 3′-extension was required for cleavage (data not shown)). Amplified DNA fragments were inserted in *Bam*HI/*Eco*RI sites of pGem-4Z. RNAs were synthesized from *Eco*RI-linearized plasmids and contained an additional 45-nt stretch of plasmid polylinker. S_I transcript, the DNA template for which has been cloned in the same manner as the variant sequences, was referred as to wild type in these experiments.

Nucleotide Sequence Accession Numbers—The nucleotide sequence for the HCV wild type genome is available in the GenBank™ data base under accession number S62220 (28). The nucleotide sequence for HCV variants presented in this article can be accessed through EMBL data base under EMBL data base accession numbers AJ248084, AJ391467, AJ391452, and AJ247989 (7).

RESULTS

Cleavage of HCV RNA Transcripts

Initial RNase P cleavage experiments involved a 554-base HCV RNA transcript (S_I nt 2486–3040). At the *top* of Fig. 1*A* is a schematic drawing of the HCV RNA genome, below which appears the S_I transcript located at the structural/nonstructural junction region. The autoradiogram in Fig. 1*B* shows that, using the S_I transcript as a substrate, RNase P peak activity alone, in the absence of any external guide sequence, cleaved the HCV transcript very efficiently, producing two intense cleavage products (5′ P_I and 3′ P_I). After this unexpected result, we wanted to assess whether cleavage was maintained in

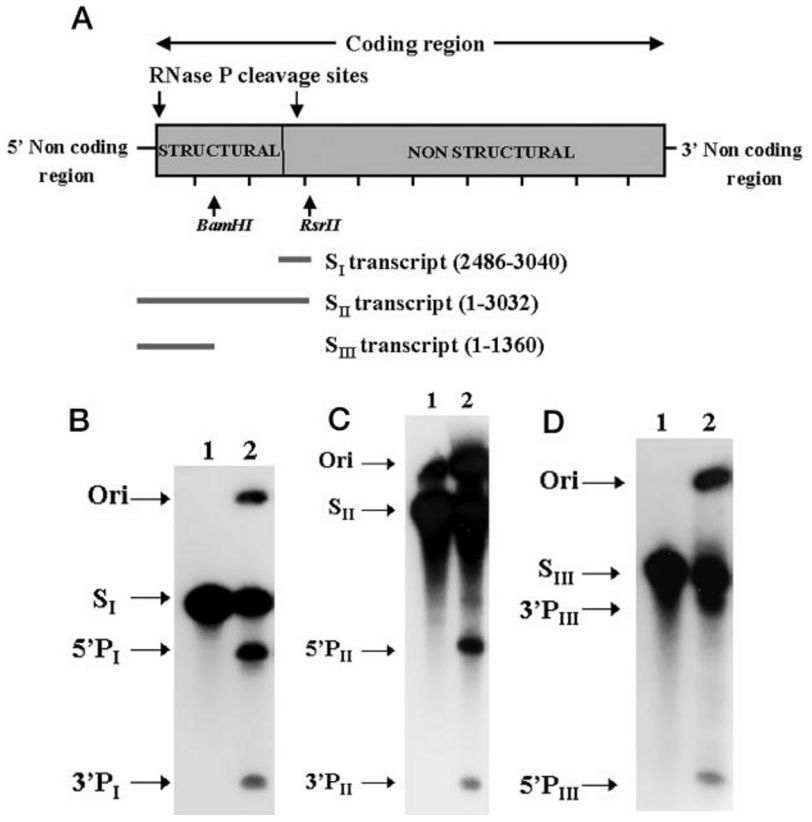

FIG. 1. **RNase P cleaves the HCV genome.** *A*, location of RNase P cleavage sites and HCV transcripts in the viral genome. S_I is a 554-nt transcript encompassing the junction fragment between structural and nonstructural regions; S_{II} covers the first one-third of the HCV genome; and S_{III} is a 1360-nt-long transcript containing the 5′-noncoding region and half of the structural region. *B–D*, autoradiograms of RNase P cleavage of S_I, S_{II}, and S_{III} transcripts, respectively. *Lane 1*, the transcript alone. The *arrows* indicate the 5′ product (5′ P) and the 3′ product (3′ P) (*lane 2*).

a larger transcript, encompassing the first one-third of the genome (Fig. 1*A*, S_{II} nt 1–3032). In the course of that demonstration, we detected a second HCV cleavage site in the IRES region (Fig. 1, *A* and *C*). Subsequently, cleavage within the IRES was confirmed using a third transcript corresponding to the first 1360 bases of HCV genome (Fig. 1*A*, S_{III} nt 1–1360) as well as in a shorter fragment, 641 nt long (S_{IV} nt 1–641).

RNase P Is Responsible for the HCV RNA Cleavages

The key experimental question of the HCV RNA cleavages obtained in the reactions involving unguided RNase P concerns a demonstration that cleavages in different sized transcripts are performed by RNase P itself and not by a co-extracted contaminant. To prove that, we have used direct and indirect methods.

Direct Method: End Group Determination and Cleavage Precision by RNA Fingerprinting

If RNase P were responsible for HCV RNA processing activity in our RNase P peak activity (HeLa cell extract), the site of cleavage might be expected to occur between precise nucleotide positions and release products containing the 3′-hydroxyl and 5′-phosphate end groups (17). Contaminating RNases almost invariably cleave to yield 5′-hydroxyl and 3′-phosphate end groups (29), and very few other RNases and ribozymes cleave the phosphodiester backbone through the same mechanism used by RNase P (30).

S_I RNA Substrate—To allow direct and precise determination of the cleavage site as well as to identify the phosphate polarity of the newly cleaved termini, substrate S_I was internally labeled either separately with α-^{32}P-labeled GTP, ATP, CTP, and UTP or simultaneously with all four labeled rNTPs and incubated with RNase P peak activity under the conditions described under "Experimental Procedures." Both cleavage products (5′ P_I and 3′ P_I) and control transcript (S_I) were fractionated by gel electrophoresis, eluted from the gel, and subjected to RNase T1 digestion. Fig. 2 shows two-dimensional fingerprint analysis (25) of the oligonucleotides generated by RNase T1 digestion of single or mixed labeled uncut S_I substrate, 5′ P_I, and 3′ P_I cleavage products and identifies the exact phosphodiester bond cleaved during the cleavage reaction to be between residues A^{2860} and G^{2861} within the four-base RNase T1-resistant oligonucleotide ^{2858}CUAG^{2861} found to be missing from both the 5′ P_I and 3′ P_I fingerprint patterns (data confirmed by secondary RNase digestion, not shown). These experiments also demonstrate that the final position of the phosphate group is 5′ to the cleavage. More precisely, the *arrow* in Fig. 2*D* indicates that a new spot appears in the GTP-labeled 3′ P_I fingerprint that does not appear in the UTP-labeled 3′ P_I (*arrow* in Fig. 2*C*). Also, it appears neither in Fig. 2, *A* and *B*, nor in the ATP- or CTP-labeled 3′ P_I fingerprints (data not shown). This novel spot was eluted and confirmed to be the 5′-terminal residue pGp by its mobility with respect to markers in secondary analysis by one-dimensional electrophoresis on DEAE and 3MM paper (26).

S_{IV} RNA Substrate—Fig. 3 depicts RNA fingerprinting analysis of the substrate S_{IV} RNA, corresponding to the HCV IRES, as well as both cleavage products generated by RNase P. In each case, T1-resistant oligonucleotides were eluted and subjected to further enzymatic characterization as described elsewhere (26). As summarized in the legend to Fig. 3, a spot (*A*, *spot 1*) from the intact S_{IV} RNA fingerprint was absent from the fingerprint pattern of both cleavage products. This missing RNase T1-resistant oligonucleotide containing the RNase P cleavage site(s) in the S_{IV} RNA substrate is the 17-mer (nt 351–367), thus indicating precise cleavage of the RNA substrate in the HCV IRES domain. This 17-mer is replaced by a new spot in each one of the cleavage products' fingerprints (Fig. 3*B*, *spot 2*; Fig. 3*C*, *spot 3*). Together, these two were found by secondary analysis to contain the sequence of the missing 17-mer with the expected composition indicating a cleavage site in

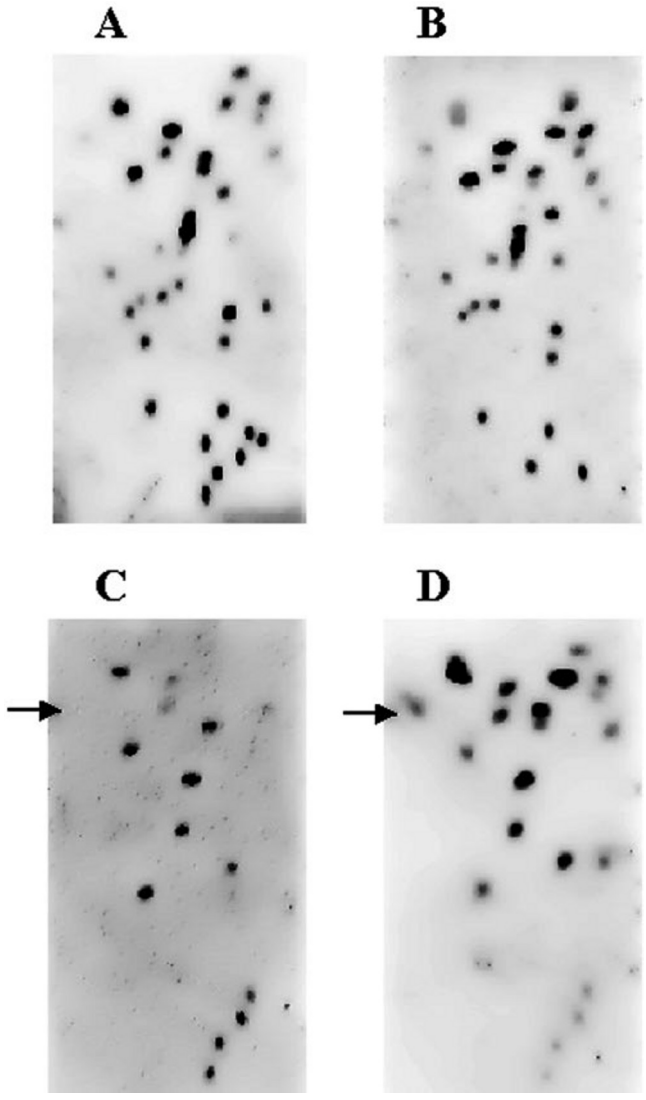

FIG. 2. **Determination of the cleavage site in the structural/nonstructural junction region.** Shown are RNase T1 fingerprints of uncut S_I labeled by all four [α-^{32}P]rNTPs containing all of the expected RNase T1-resistant oligonucleotide spots between residues 2486 and 3040 (*A*), 5′ P_I labeled by all four [α-^{32}P]rNTPs containing spots that correspond to nucleotides 2486–2857 (*B*), and 3′ P_I labeled by [α-^{32}P]rUTP or [α-^{32}P]rGTP, respectively, containing the expect spots that correspond to residues 2862–3040 (data confirmed by secondary analysis of eluted spots) (*C* and *D*). The *arrows* in *C* and *D* indicate the positions of RNase T1-generated pGp from 3′ P_I.

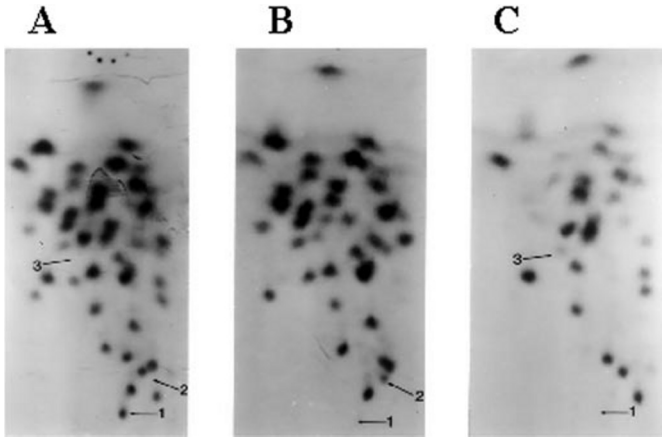

FIG. 3. **Mapping the cleavage site in the 5′ region.** *A*, RNase T1 fingerprints of uncut substrate containing HCV bases 1–641, transcribed from DNA template cleaved with *Sac*II, labeled by all four [α-^{32}P]rNTPs. This pattern contains all of the expected RNase T1-resistant oligonucleotide spots as determined by secondary analysis (25). Spot 1, containing the 17-base RNase T1-resistant product AAUCCUAAACCUCAAAG, is indicated, along with positions 2 and 3, which are unoccupied in this *panel*. ***B*,** product labeled as in *A*, containing spots corresponding to bases 1–361/362. Spot 1 is missing, and spot 2, which has the sequence AAUCCUAAACC (bases 351–361) or AAUCCUAAACCU (bases 351–362), is present instead. Spot 2 was identified by secondary analysis, but its 3′-end could not be identified beyond the conclusion that it is either C^{361} or U^{362}. *C*, 3′ product labeled as in *A*, containing spots corresponding to bases 364–641. Spot 1 is missing, and spot 3, which has the sequence *X*AAAG (362/363–367, where *X* represents C or UC), is present instead. Spot 3 was identified by secondary analysis and must have one or two additional bases upstream from the AAAG motif (bases 364–367), which are not yet identified. Further experiments are in progress to pin down exact termini within this RNase P cleavage domain.

the vicinity of bases 361–363. Further experiments are in progress to pin down exact termini within this RNase P cleavage domain.

Indirect Methods: Immunoprecipitation and Competitive Inhibition

Two indirect strategies were used to demonstrate that the activity that cleaves S_I and S_{II} and exactly co-purified with RNase P peak activity was in fact RNase P. The experiments were carried out using S_I, S_{II}, and S_{III} as substrates.

Immunoprecipitation—Some patients with autoimmune diseases produce antibodies against a 38–40-kDa protein (designated Th antigen) which is an integral component of eukaryotic RNase P (27). In the immunoprecipitation experiment, we have incubated a serum containing anti-Th antibodies with our peak activity (RNase P extract), and we have assayed both the supernatant and the pellet. The anti-Th serum that immunodepleted pre-tRNA^{Tyr} cleavage activity from our glycerol gradient-purified enzyme (Fig. 4*A*, *lane 2*) also immunodepleted cleavage of HCV transcripts (Fig. 4, *B*, *lanes 6–8*, and *C*, *lanes 22–24*). Moreover, the autoimmune serum was able to precipitate the processing activity of HCV transcripts S_I and S_{II} (Fig. 4, *B*, *lanes 9–11*, and *C*, *lanes 25–27*) as well as pre-tRNA^{Tyr} (Fig. 4*A*, *lane 3*) and a human suppressor pre-tRNA (data not shown). In contrast, the normal human serum failed to precipitate the processing activity (Fig. 4, *B*, *lanes 16–18*, *C*, *lane 21*). Control reactions of RNase P cleavage, using protein A-Sepharose beads with no added antiserum, showed that the cleavage activity remains in the supernatant after the immunoprecipitation and is not found in the pellet (Fig. 4*B*, *lanes 5* and *12*). An inverse correlation between the percentage of cleavage with increasing anti-Th sera (Fig. 4*C*, *lanes 25–27*) may be due to inactivation of RNase P activity due to the presence of polyclonal antibodies reacting with important motifs for substrate recognition.

Competitive Inhibition—Like RNase P, MRP RNases cleave RNA to generate 5′-phosphate and 3′-hydroxyl termini (31) and may be immunoprecipitated with anti-Th serum. As a distinguishing feature, MRP RNase does not cleave pre-tRNA^{Tyr} (32). To rule out the possibility that MRP enzymes were responsible for HCV cleavage, we carried out competitive inhibition experiments between HCV RNA and pre-tRNA. The experiments consisted of incubating the same amount of HCV RNA (S_I, S_{II}, or S_{III}) with increasing concentrations of pre-tRNA (from ⅛-fold to 4-fold) to inhibit HCV RNA cleavages. When labeled pre-tRNA^{Tyr} was included in the S_I HCV cleavage reactions, the amount of HCV cleavage product decreased with an increasing competitor concentration at a ratio near 1:1 (Fig. 5*A*, *lane 5*). With the long transcript (S_{II}), a decrease of products from the two cleavage reactions was more noticeable

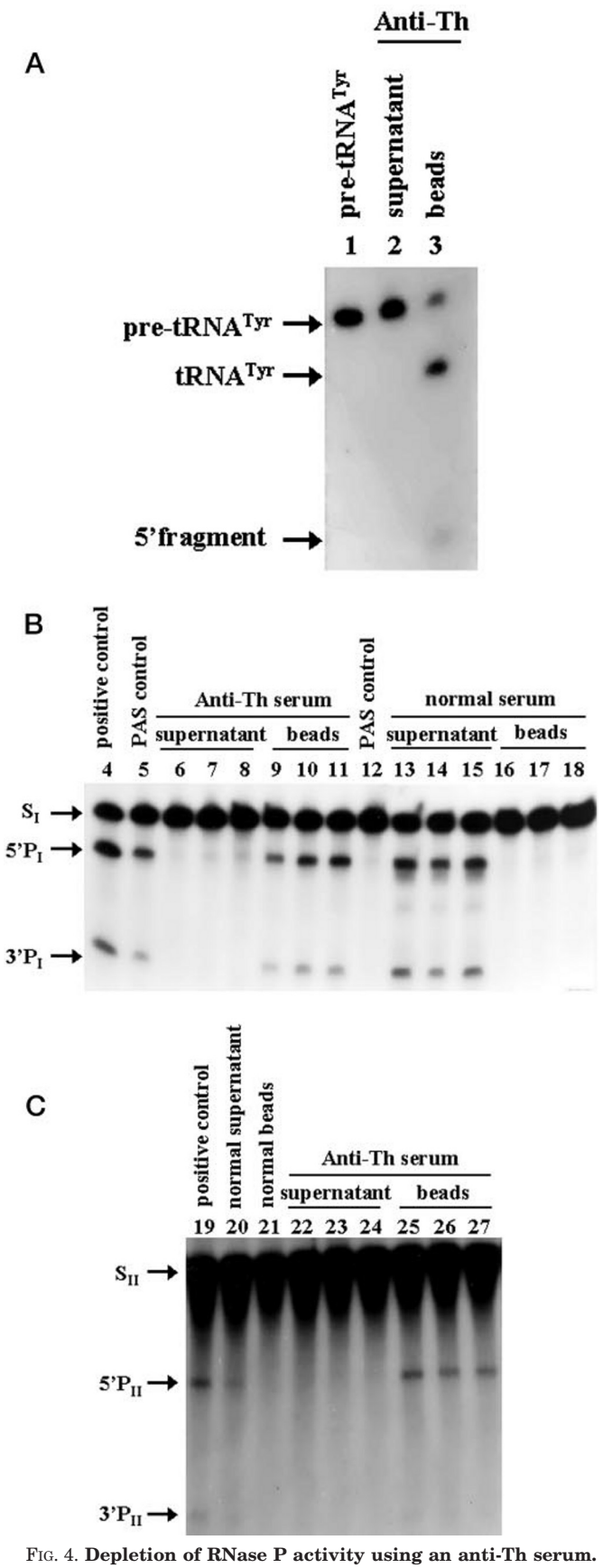

FIG. 4. **Depletion of RNase P activity using an anti-Th serum.** Shown are cleavage reactions of three different substrates, bacterial pre-tRNA^{Tyr} (*A*), S_I transcript (*B*), and S_{II} transcript (*C*), incubated with immunoprecipitate from beads coated with 0.5 μl (*lane 3*) and increasing concentrations (0.25, 0.5, and 1 μl) of either anti-Th serum (*lanes 9–11* and *25–27*) or normal human serum (*lanes 16–18*). Supernatant from beads coated with 0.5 μl (*lane 2*) and the same previous three concentrations of anti-Th serum (*lanes 6–8* and *22–24*) or normal serum (*lanes 13–15*) were also used to incubate the transcript. Only the intermediate concentration of normal serum (*lanes 20* and *21*) was tested with S_{II} transcript. *Lanes 5* (supernatant) and *12* (beads) are controls showing the lack of affinity between Protein A-Sepharose beads and RNase P without anti-Th serum addition. *Lane 1*, pre-tRNA alone; *lanes 4* and *19*, standard reactions used as positive controls.

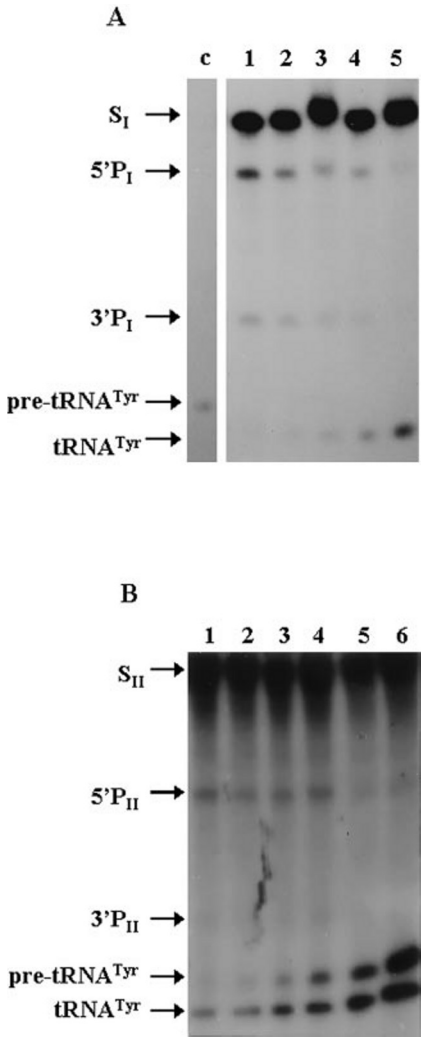

FIG. 5. **Pre-tRNA^{Tyr} competes with and inhibits the RNase P-specific cleavage of HCV RNA.** Shown are autoradiograms of the cleavage of S_I transcript (*A*) and S_{II} transcript (*B*) by RNase P in the presence of increasing concentrations of pre-tRNA^{Tyr}. *Lane C*, pre-tRNA alone; *lanes 1–5*, cleavage reactions using a constant concentration of S_I or S_{II} transcript (1.8 nM) and increasing concentrations of pre-tRNA (0.225, 0.45, 0.9, 1.8, and 3.6 nM, respectively). An additional assay using 7.2 nM pre-tRNA^{Tyr} (*lane 6*) is shown in *B*.

when the molar ratio between pre-tRNA^{Tyr} and S_{II} reached 2:1 (Fig. 5*B*).

RNase P Cleaves HCV Variants

The direct consequence of the high mutation rate in HCV replication is that variant genomes are continuously being generated. Thus, multiple variant sequences (quasispecies) cocirculate within a patient, and each patient carries a virus with a distinct "master" (the most frequent) sequence (5, 10). To define cleavage by RNase P as a general property of HCV, four viral sequences obtained from different patients, together with S_I sequence (referred to as wild type here), were compared for RNase P cleavage accessibility (Fig. 6*A*). We used transcripts from cloned HCV PCR fragments, representing the master

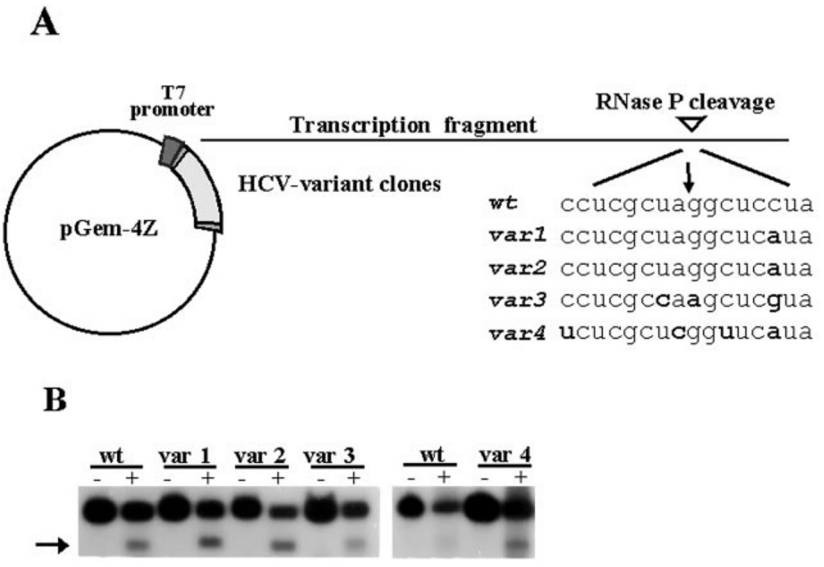

FIG. 6. **RNase P cleavage of HCV 2658–2869 RNA variants.** *A*, schematic representation of HCV variants cloned in a transcription vector. The *open arrowhead* indicates RNase P cleavage site in the RNA sequence. Wild type (*wt*) corresponds to S_I transcript. The 8-nt flanking the cleavage site of wild type and variant sequences are shown *below*. *B*, autoradiograms show the RNase P-specific cleavage of four different HCV variant and wild type RNAs. +, presence of RNase P in the reaction. The 5′ cleavage products are indicated by an *arrow*.

sequence from infected patients' quasispecies, with mutations at the vicinity or exactly at the nucleotides adjacent to the scissile bond in the structural/nonstructural junction. Cleavage was consistently observed in all sequences tested although with different efficiencies (Fig. 6*B*).

HCV RNA Competes with RNase P Cleavage of Pre-tRNA

The concept of RNA mimicry has been defined for those cases where the structure of an RNA molecule has evolved to fit a binding site on a protein or a macromolecular complex that normally interacts with a different RNA (33). The specific cleavage of HCV RNA by RNase P suggests that the viral RNA has structural similarities to tRNA. We wished to assess how much these HCV RNA structures resemble tRNA. In competition experiments reciprocal to those shown in Fig. 5, we tested the ability of HCV RNA transcripts S_I and S_{III} (0.9–180 nM) to compete for RNase P activity with the natural substrate pre-$tRNA^{Tyr}$ (1.8 nM). Fig. 7 shows that by using an RNase P concentration capable of cleaving around 25% of the pre-$tRNA^{Tyr}$ in the reaction, the amount of pre-tRNA cleavage products decreased with increasing HCV RNA concentration. The amount of HCV RNAs required for half-inhibition were between 4- and 6-fold molar excess and were similar for both S_I and S_{III}. In contrast, similar amounts of an unrelated RNA of 400-nt length corresponding to hepatitis B virus (HBV) surface antigen mRNA (nt 1400–1800 of HBV *adr* subtype) (34), which is not cleaved by RNase P, had no observable effect on RNase P activity on pre-tRNA (data not shown). The fact that the HCV RNA is a competitive inhibitor of pre-tRNA cleavage within a 1 order of magnitude range is evidence of molecular mimicry between the HCV RNA motifs at the cleavage sites and those in pre-tRNA. Furthermore, the inhibition of pre-tRNA cleavage provides strong evidence that the interaction of HCV RNA is with RNase P and not with RNase MRP, in agreement with our previous conclusion that RNase P is responsible for HCV RNA cleavage.

The results shown in Figs. 2 and 3, which were first completed using RNAs produced and cleaved in the Barcelona laboratory, have also been repeated in the New York laboratory. These experiments were repeated using two different preparations of human RNase P (from Dr. Sidney Altman), and the same results were reproduced.

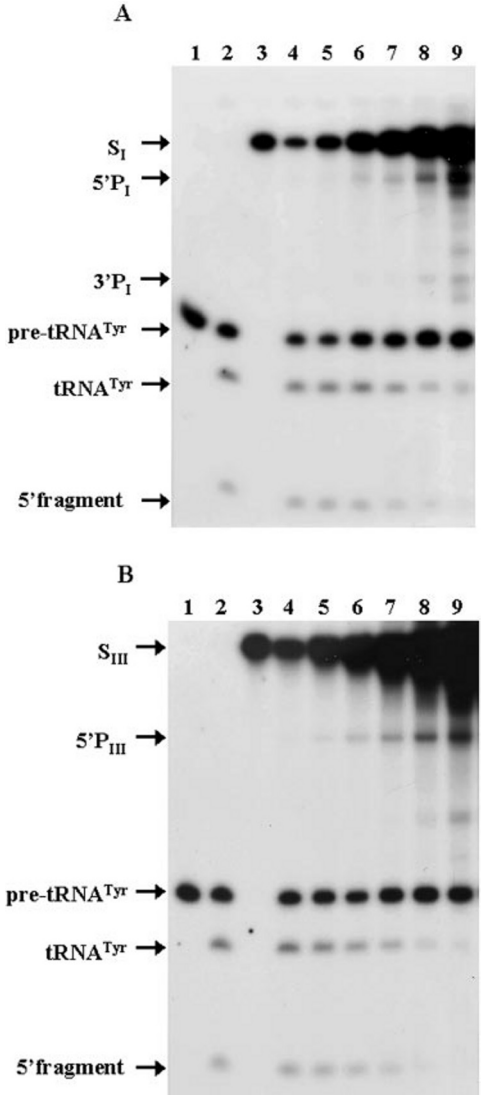

FIG. 7. **Competitive inhibition of pre-tRNA processing by the HCV RNA.** *A*, *lanes 4–8*, different amounts of S_I transcript (0.9, 1.8, 3.6, 7.2, 14.4, and 28.8 nM) were premixed with 1.8 nM of pre-$tRNA^{Tyr}$ transcript and incubated with RNase P. In all of the reactions, a concentration of RNase P able to cut the 20–30% pre-$tRNA^{Tyr}$ alone in 30 min was used (*lane 2*). *Lane 1*, pre-$tRNA^{Tyr}$ alone. ***B*,** the same protocol as in *A* was carried out with S_{III} transcript.

DISCUSSION

We have defined a new specific interaction *in vitro* between HCV RNA and a host component, RNase P, and we have

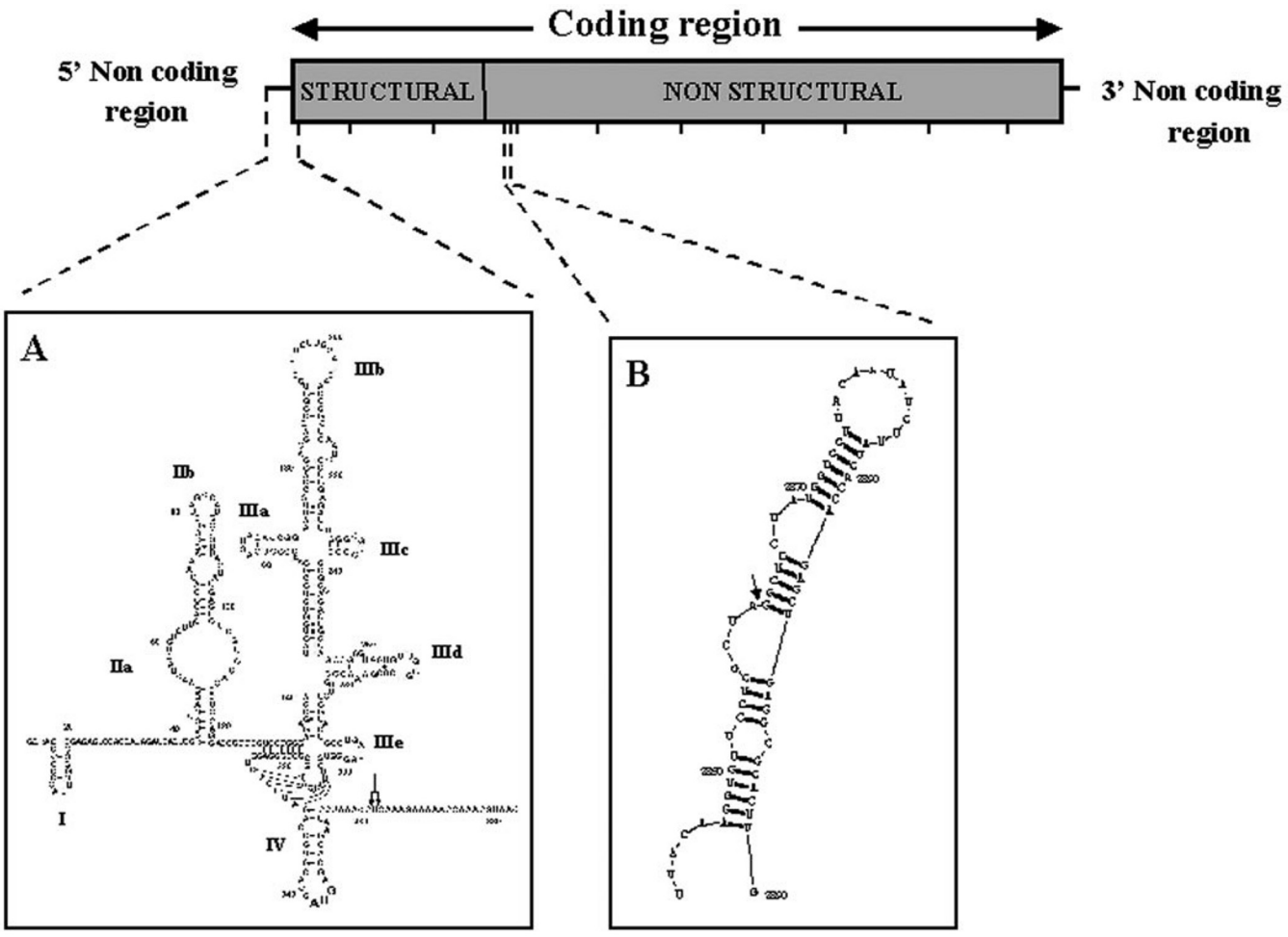

FIG. 8. **Positioning of the two RNase P cleavage sites on the predicted secondary structure model for the HCV RNA.** HCV genome is represented schematically, and the putative structures of domains containing the two RNase P cleavages sites are drawn. *A*, the 5′-noncoding region containing the IRES domain (nt 1–383) is shown as the currently accepted structure, including the redrawing of domain II (47) and the predicted pseudoknot structure in domain IV. The *two arrows* indicate the RNase P cleavage site in the vecinity of bases 361–363. *B*, the structure of a 70-nt portion (nt 2841–2890) of the folded structural/nonstructural junction region, predicted by *RNA Structure*, version 3.5, is represented. The *single arrow* indicates the exact position of human RNase P cleavage.

confirmed that HCV RNA transcripts act as competitive inhibitors of pre-tRNA^{Tyr} processing. This represents evidence for a similarity in structure and/or function between both accessible motifs in HCV RNA and tRNA molecules.

RNase P specifically cleaves pre-tRNA in all organisms to produce mature 5′-ends. There have been questions raised about the universal significance of RNase P cleavage in non-tRNA molecules, especially concerning yeast RNase P. Chamberlain *et al.* (35) have suggested that yeast RNase P can sometimes cleave 5.8 S rRNA at sites that lack properties normally associated with canonical tRNA. Given the uncertain evolutionary history of this rRNA species, however, it is hard to prove or disprove the acquisition of internal tRNA-like domains, which are in fact present in analogous prokaryotic spacer regions of rRNA precursors. It is also the case that RNase P cleavage has reliably identified a number of authenticated tRNA-like domains in non-tRNA molecules, including bacterial SRP and tmRNAs and various plant viral RNA genomes (36–40). Given that our two HCV domains undergo RNase P cleavage with the same efficiency as pre-tRNA, we believe that such recognition by RNase P is an indication for the presence of two possible tRNA-like structures in the HCV genome.

The ability to mimic tRNA as we observe here in HCV RNA was first discovered 30 years ago at the 3′-end of the turnip yellow mosaic virus because of its ability to undergo covalent linkage with amino acids catalyzed by aminoacyl-tRNA synthetase (41). Subsequently, this and other plant viral RNAs were seen to be accessible to a battery of factors involved in other tRNA-related activities (including accessibility of bacterial RNase P) (37, 41, 42). Nevertheless, *in vivo* functional mimicry was not complete, since viral RNAs were not amino acid donors for protein synthesis but rather participated in virus replication.

This proposed idea is further supported by the presence of a pseudoknot near the HCV IRES (43) cleavage site (a common element in tRNA-like structures including that which is known to interact with *E. coli* RNase P in the case of the tRNA-like motifs of plant viral RNAs) (42) (Fig. 8). Such a structure might contribute to the recruitment of the translational machinery in the absence of a 5′-terminal cap. A recent study by J. R. Lytle *et al.* (44) confirms that this pseudoknot domain of the HCV IRES is among those protected from extensive pancreatic RNase A digestion by initiating 80 S ribosomes.

During protein elongation, this RNA structure might also help a ribosomal frameshift, which has been described to happen within cleavage boundaries and generates a new antigen in HCV-infected patients (45, 46).

Concerning the internal cleavage site, the predicted secondary structure formed by the RNA sequence flanking the cleav-

age site (the cleavage is 5′ to a G residue (G^{2861}) and is followed by two helices totaling 13 bases connected through a bulge (predicted by *RNA Structure*, version 3.5)) is in agreement with the characteristic features of the minimal model substrate for human RNase P (21) (Fig. 8). In particular, cleavage determinants are confined to the tRNA domain that contains the acceptor stem, the T stem and loop, and the junction between them (21), a recognition feature also shared by the *E. coli* elongation factor EFTu (33). Also, the internal HCV RNase P cleavage site resides in a highly structured domain of the viral RNA (data not shown), which might be also compatible with a tRNA structure. Nevertheless, there is no readily obvious functional explanation for such a structure at this site.

The presence of HCV RNA in the nucleus (where most RNase P is found) has not been demonstrated (48), and no evidence of subgenomic HCV RNAs has been reported (49), arguing against an active role of RNase P cleavage in HCV biology. Whatever the role of the RNase P-sensitive structures, their importance for virus viability is apparent, despite the notorious heterogeneity and dynamics of change in HCV quasispecies within the infected patient. A cleavage site at residue A^{2860}, present in the master sequences from individual patients (differing at or near the position of cleavage), should be interpreted in a context where variants arise continuously and are repeatedly subjected to competition pressures. Thus, the relative success of a mutant is the result of its ability to replicate. This strongly suggests that (i) the RNA structure that confers accessibility to RNase P is not affected by mutations that become fixed within the cleavage boundaries during error-prone replication, and (ii) there is a continuous selective advantage for the sequences within the quasispecies carrying the RNase P-accessible structure. Moreover, conservation of RNase P-cleavable structures in the genomes of different patients implies that this structure is even conserved during genetic bottlenecking of HCV quasispecies during host-to-host transmission, despite the fact that this area is one of the most variable regions of the HCV genome at the nucleotide sequence level (6). Altogether, this makes RNase P cleavability an inherent property of HCV.

Higher order structures of RNA play functional roles, and the mutations that alter such higher order structures must be subjected to negative selection. Such a strong tendency to maintain RNase P-sensitive structures within the viral genome might be important in the development of therapeutic strategies against the virus because they can represent highly susceptible targets for *E. coli* RNase P M1 RNA (22, 23).

The next phase of this work will involve investigation of the minimum requirements for cleavage at both the IRES and internal site. Minimal length substrates will serve to define to what extent tRNA processing enzymes like aminoacyl-tRNA synthetase, tRNA nucleotidyl transferase, tRNA methyltransferases, and interacting factors (iEF2 and EF-1) react with these HCV motifs. Comparison of such results at the two HCV RNase P cleavage sites should help us to understand in greater detail HCV substrate structure, tRNA mimicry, rules underlying recognition by human RNase P, and, in the particular case of the IRES motif, possible participation in translation.

Acknowledgments—We thank Drs. C. Gelpí and J. L. Rodriguez from the Servei d'Immunologia, Hospital Sant Pau (Barcelona, Spain) for providing the autoimmune serum. An HCV clone was kindly provided by Drs. M. Honda and S. Lemon, and tRNA precursors and RNase P were from Drs. S. Altman and C. Guerrier-Takada. We also thank Dr. E. Martinez-Salas for critical reading of the manuscript.

REFERENCES

1. Houghton, M. (1996) in *Fields' Virology* (Fields, B. N., Knipe, D. N., and Howley, P. N., eds) pp. 1035–1057, Lippincott-Raven, Philadelphia
2. Tsukiyama-Kohara, K., Iizuka, N., Kohara, M., and Nomoto, A. (1992) *J. Virol.* **66,** 1476–1483
3. Houghton, M., Selby, M., Weiner, A., and Choo, Q. L. (1994) *Curr. Stud. Hematol. Blood Transfus.* 1–11
4. Han, J. H., Shyamala, V., Richman, K. H., Brauer, M. J., Irvine, B., Urdea, M. S., Tekamp-Olson, P., Kuo, G., Choo, Q. L., and Houghton, M. (1991) *Proc. Natl. Acad. Sci. U. S. A.* **88,** 1711–1715
5. Martell, M., Esteban, J. I., Quer, J., Genesca, J., Weiner, A., Esteban, R., Guardia, J., and Gomez, J. (1992) *J. Virol.* **66,** 3225–3229
6. Bukh, J., Miller, R. H., and Purcell, R. H. (1995) *Semin. Liver Dis.* **15,** 41–63
7. Cabot, B., Martell, M., Esteban, J. I., Sauleda, S., Otero, T., Esteban, R., Guardia, J., and Gomez, J. (2000) *J. Virol.* **74,** 805–811
8. Domingo, E., and Holland, J. J. (1994) in *Evolutionary Biology of Viruses* (Morse, S. S., ed) pp. 161–184, Raven Press, New York
9. Domingo, E., and Holland, J. J. (1997) *Annu. Rev. Microbiol.* **51,** 151–178
10. Gomez, J., Martell, M., Quer, J., Cabot, B., and Esteban, J. I. (1999) *J. Viral Hepat.* **6,** 3–16
11. Poynard, T., Marcellin, P., Lee, S. S., Niederau, C., Minuk, G. S., Ideo, G., Bain, V., Heathcote, J., Zeuzem, S., Trepo, C., and Albrecht, J. (1998) *Lancet* **352,** 1426–1432
12. Enomoto, N., Kurosaki, M., Tanaka, Y., Marumo, F., and Sato, C. (1994) *J. Gen. Virol.* **75,** 1361–1369
13. Le Guen, B., Squadrito, G., Nalpas, B., Berthelot, P., Pol, S., and Brechot, C. (1997) *Hepatology* **25,** 1250–1254
14. Polyak, S. J., McArdle, S., Liu, S. L., Sullivan, D. G., Chung, M., Hofgartner, W. T., Carithers, R. L., Jr., McMahon, B. J., Mullins, J. I., Corey, L., and Gretch, D. R. (1998) *J. Virol.* **72,** 4288–4296
15. Plehn-Dujowich, D., and Altman, S. (1998) *Proc. Natl. Acad. Sci. U. S. A.* **95,** 7327–7332
16. Altman, S. (1995) *Bio/Technology* **13,** 327–329
17. Robertson, H. D., Altman, S., and Smith, J. D. (1972) *J. Biol. Chem.* **247,** 5243–5251
18. Altman, S. (1989) *Adv. Enzymol. Relat. Areas Mol. Biol.* **62,** 1–36
19. Guerrier-Takada, C., Gardiner, K., Marsh, T., Pace, N., and Altman, S. (1983) *Cell* **35,** 849–857
20. Bartkiewicz, M., Gold, H., and Altman, S. (1989) *Genes Dev.* **3,** 488–499
21. Yuan, Y., and Altman, S. (1995) *EMBO J.* **14,** 159–168
22. Kilani, A. F., Trang, P., Hsu, J. S., Kim, J., Nepomuceno, E., Liou, K., and Liu, F. (2000) *J. Biol. Chem.* **14,** 10611–10622
23. Liu, F., and Altman, S. (1995) *Genes Dev.* **9,** 471–480
24. Martell, M., Gómez, J., Esteban, J. I., Sauleda, S., Quer, J., Cabot, B., Esteban, R., and Guardia, J. (1999) *J. Clin. Microbiol.* **37,** 327–332
25. Branch, A. D., Benenfeld, B. J., and Robertson, H. D. (1989) *Methods Enzymol.* **180,** 130–154
26. Barrell, B. G. (1971) in *Procedures in Nucleic Acid Research* (Cantoni, G. L., and Davies, D. R., eds) Harper and Row, New York
27. Eder, P. S., Kekuda, R., Stolc, V., and Altman, S. (1997) *Proc. Natl. Acad. Sci. U. S. A.* **94,** 1101–1106
28. Hayashi, N., Higashi, H., Kaminaka, K., Sugimoto, H., Esumi, M., Komatsu, K., Hayashi, K., Sugitani, M., Suzuki, K., and Tadao, O. (1993) *J. Hepatol.* **17,** Suppl. 3, 94–107
29. Adams, R. L. P., Knowler, J. T., and Leader, D. P. (1992) in *The Biochemistry of the Nucleic Acids*, pp. 97–133, Chapman and Hall Ltd., London
30. Pyle, A. M. (1993) *Science* **261,** 709–714
31. Chang, D. D., and Clayton, D. A. (1987) *EMBO J.* **6,** 409–417
32. Karwan, R., Bennett, J. L., and Clayton, D. A. (1991) *Genes Dev.* **5,** 1264–1276
33. Springer, M., Portier, C., and Grunberg-Manago, M. (1998) in *RNA structure and function* (Simons, R. W., ed) pp. 337–413, Cold Spring Harbor Laboratory Press, Cold Spring Harbor, NY
34. Ono, Y., Onda, H., Sasada, R., Igarashi, K., Sugino, Y., and Nishioka, K. (1983) *Nucleic Acids Res.* **11,** 1747–1757
35. Chamberlain, J. R., Pagàn-Ramos, L., Kindelberger, D. W., and Engelke, D. R. (1996) *Nucleic Acids Res.* **24,** 3158–3166
36. Peck-Miller, K., and Altman, S. (1991) *J. Mol. Biol.* **221,** 1–5
37. Guerrier-Takada, C., van Belkum, A., Pleij, C. W., and Altman, S. (1988) *Cell* **53,** 267–272
38. Baumstark, T., and Ahlquist, P. (2001) *RNA* **11,** 1652–1670
39. Joshi, S., Chappeville, F., and Haenni, A. L. (1982) *Nucleic Acids Res.* **10,** 1947–1962
40. Komine, Y., Kitabatke, M., Yokogawa, T., Nishikawa, K., and Inokuchi, H. (1994) *Proc. Natl. Acad. Sci. U. S. A.* **91,** 9223–9227
41. Giegé, R., Florentz, C., and Dreher, T. W. (1993) *Biochimie* (*Paris*) **75,** 569–582
42. Mans, R., Guerrier-Takada, C., Altman, S., and Pleij, C. (1990) *Nucleic Acids Res.* **18,** 3479–3487
43. Wang, C., Le, S. Y., Ali, N., and Siddiqui, A. (1995) *RNA* **1,** 526–537
44. Lytle, J. R., Wu, L., and Robertson, H. D. (2001) *J. Virol.* **75,** 7629–7636
45. Walewsky, J. L., Keller, T. B., Stump D, D., and Branch, A. D. (2001) *RNA* **20,** 3840–3848
46. Xu, Z., Choi, J., Yen, T. S., Lu, W., Stoecher, A., Govindarajan, S., Chien, D., Selby, M. J., and Ou, J.-H. (2001) *EMBO J.* **20,** 3840–3848
47. Lyons, A. J., Lytle, J. R., Gómez, J., and Robertson, H. D. (2001) *Nucleic Acids Res.* **29,** 2535–2541
48. Bartenschlager, R., and Lohmann, V. (2000) *J Gen. Virol.* **81,** 1631–1648
49. Moradpour, D., Kary, P., Rice, C. M., and Blum, H. E. (1998) *Hepatology* **28,** 192–201